



Shear flow of sphere packings in the geometric limit

Pierre-Emmanuel Peyneau, Jean-Noël Roux

► To cite this version:

Pierre-Emmanuel Peyneau, Jean-Noël Roux. Shear flow of sphere packings in the geometric limit. The XVth International Congress on Rheology (The Society of Rheology 80th Annual Meeting), Aug 2008, Monterey, United States. pp.947-949, 10.1063/1.2964904 . hal-00531796

HAL Id: hal-00531796

<https://hal.science/hal-00531796>

Submitted on 3 Nov 2010

HAL is a multi-disciplinary open access archive for the deposit and dissemination of scientific research documents, whether they are published or not. The documents may come from teaching and research institutions in France or abroad, or from public or private research centers.

L'archive ouverte pluridisciplinaire **HAL**, est destinée au dépôt et à la diffusion de documents scientifiques de niveau recherche, publiés ou non, émanant des établissements d'enseignement et de recherche français ou étrangers, des laboratoires publics ou privés.

Shear flow of sphere packings in the geometric limit

P.-E. Peyneau and J.-N. Roux

UR Navier, Université Paris-Est, 2 allée Kepler, F-77420 Champs-sur-Marne, France

Abstract. We investigate the behavior of a model granular material made of frictionless, nearly rigid equal-sized beads, in the quasistatic limit, by numerical simulation. In the *macroscopic geometric* limit (that is the macroscopic, rigid and quasistatic limits), with either volume or normal stress controlled simulations, static and dynamic macroscopic friction coefficients coincide, dilatancy vanishes and the material satisfies a Lade-Duncan failure criterion. The macroscopic shear strength stems from both contact network and force anisotropy.

Keywords: granular matter, suspensions, frictionless particles, quasistatic, yield, molecular dynamics

PACS: 45.70.-n, 83.80.Hj, 81.40.Lm, 83.10.Rs

INTRODUCTION

Frictionless bead packings are elusive systems that have seldom been studied *per se* [1, 2]. Most studies of granular systems involve a nonzero intergranular friction coefficient, as in real granular materials, and the frictionless case is rarely treated. However, the study of this limit may prove valuable. For instance, highly concentrated non-Brownian suspensions may be modeled as assemblies of nearly touching grains bonded by a viscous lubricant that penalizes the relative normal motion of two particles compared to a relative tangential motion: ideal lubrication effectively suppresses the tangent forces. Thus, a model material made of frictionless beads should be able to account for the behavior of a dense suspension in the quasistatic limit. Furthermore, frictionless assemblies only involve a limited number of parameters and incorporate basic geometric effects also shared by dry granular materials and suspensions. This is the reason why we investigate the macroscopic behavior of frictionless assemblies of grains and its microscopic origin.

MATERIAL AND NUMERICAL EXPERIMENTS

We consider packings of equal-sized spherical beads of diameter a and mass m , enclosed in a cuboidal simulation cell. Beads interact through their contacts: the force transmitted is purely normal and is the sum of an Hertzian elastic term $F_N^e = \tilde{E}\sqrt{a}h^{3/2}/3$ (h is the normal elastic deflection, $\tilde{E} \equiv E/(1 - \nu^2)$ where E is the Young modulus of the material the beads are made of, and ν its Poisson ratio) and of a viscous term $F_N^v = \zeta(m\tilde{E})^{1/2}(ah)^{1/4}\dot{h}$ (ζ is the level of viscous damping) entailing a velocity-independent restitution coefficient $e_N(\zeta)$ in binary collisions.

We use different molecular dynamics (MD) procedures in which some strain, or strain rate, and stress components are externally imposed to an initial state, resulting from the isotropic compression of a granular gas (the initial state is thus a random close packing), to simulate the bulk of the system and to determine the intrinsic constitutive laws [3].

Once suitably expressed in dimensionless form, all results depend on four dimensionless parameters: the level of viscous damping ζ (which becomes irrelevant in the quasistatic limit), the inertia number $I = \dot{\gamma}(m/(aP))^{1/2}$ and the stiffness number $\kappa = (\tilde{E}/P)^{2/3}$, and possibly the number of particles N . We are primarily interested in the macroscopic geometric limit (*i.e.* the triple limit of $N \rightarrow +\infty$, $I \rightarrow 0$ and $\kappa \rightarrow +\infty$). Note that this limit is very challenging since the number of MD time steps required to reach a shear strain γ is proportional to $\gamma N \kappa^{1/2} I^{-1}$.

MACROSCOPIC BEHAVIOR

First, we focus our attention on *rate-controlled shear simulations*. After a certain amount of shear, the system reaches a steady state where no enduring shear localization is observed. Thus, constitutive laws can be found by averaging on time and on the whole sample. This is done thanks to an accurate tool (the so-called blocking method) allowing to

extract from a steady time series an average and a significant error on it. The inertia number I has the most important impact on the system behavior (see Fig. 1). κ and N have almost no effect on the dynamic macroscopic friction coefficient $\mu^* = |\sigma_{12}|/|\sigma_{22}|$, and μ^* hardly evolves with ζ for $I < 0.01$. ζ has also hardly any effect on the average volume fraction Φ for $I < 0.01$, but Φ is affected by κ (cf. Fig. 1) and is a slightly increasing function of N . $\Phi \simeq 0.64$ in the quasistatic limit. Results obtained are independent of the initial configuration.

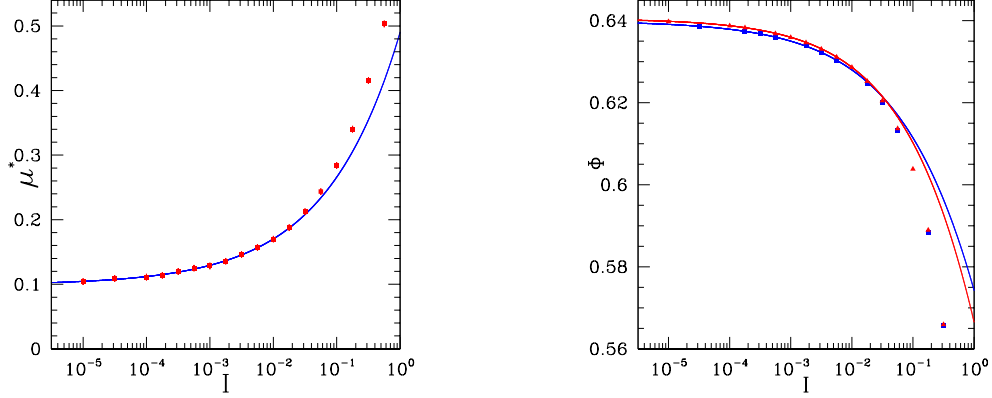


FIGURE 1. Left: μ^* as a function of I , fitted by $\mu^*(I \rightarrow 0) + cI^\alpha$ with $\mu^*(I \rightarrow 0) = 0.101 \pm 0.004$ in the geometric limit. Right: Φ as a function of I for $\kappa = 3.9 \times 10^4$ (blue squares) and $\kappa = 8.4 \times 10^3$ (red triangles). Error bars are smaller than symbols.

We checked that the kind of boundary conditions employed has no importance. Fig. 2 shows that fixed-volume simulations lead to the same results we obtained with normal stress-controlled calculations, but with much more stronger fluctuations. Fluctuations of the measured quantities were observed to vanish for $N \rightarrow +\infty$ and both methods should be equivalent in this limit. However, in the case of a finite-size sample, extracting an accurate information from a stress driven numerical experiment is easier than analyzing the results provided by a fixed-volume computation.

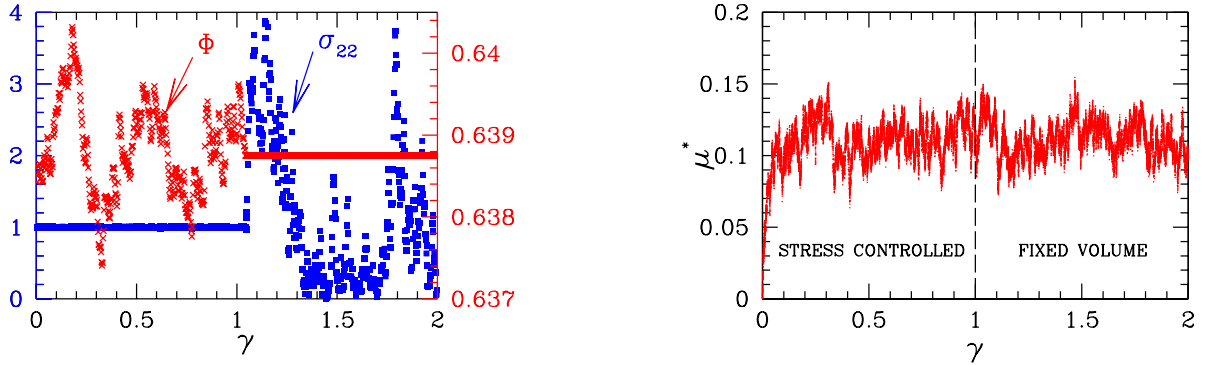


FIGURE 2. Left: σ_{22} (blue squares) and Φ (red crosses) as functions of the deformation γ . Right: macroscopic friction μ^* as a function of γ . The simulation is stress-controlled for $\gamma < 1$ and volume-controlled for $\gamma > 1$.

Previous results coincide with those obtained with *static shear simulations*, where increasing values of shear stress τ are stepwise applied to an initially isotropic configuration. For each value of τ , one waits until a satisfactory equilibrium state is reached. The calculation is stopped if the packing does not equilibrate after 5×10^7 MD time steps and the largest value τ for which an equilibrium state was obtained is kept as an estimate of the shear stress threshold for onset of flow. Static shear simulations show that the static macroscopic friction coefficient $\mu^{\text{stat}} \equiv |\tau_{\text{max}}|/P$, computed as an average on a few configurations, is size dependent. However, in the macroscopic geometric limit, it is equal to 0.091 ± 0.009 and coincides with $\mu^*(I \rightarrow 0) = 0.101 \pm 0.004$. These numerical experiments also confirm that frictionless bead assemblies do not display any dilatancy in the macroscopic geometric limit. The volume fraction of the system remains equal to Φ_{RCP} under a stress deviator.

In order to study the failure criterion of the material, triaxial compression and extension tests have also been performed. Since there is no stress scale in the problem, the yield surface has necessarily a conical shape whose axis is the trisectrix in the stress space. Fig. 3 shows that the Mohr-Coulomb model is not adequate whereas the Lade-Duncan

model, given by $f_{LD}(\underline{\underline{\sigma}}) = (\text{tr} \underline{\underline{\sigma}})^3 / \det \underline{\underline{\sigma}} - k \leq 0$, describes well the experimental failure criterion. The parameter k depends on N (see Fig. 3) in the geometric limit and is approximately equal to 27.15 in the $N \rightarrow +\infty$ limit.

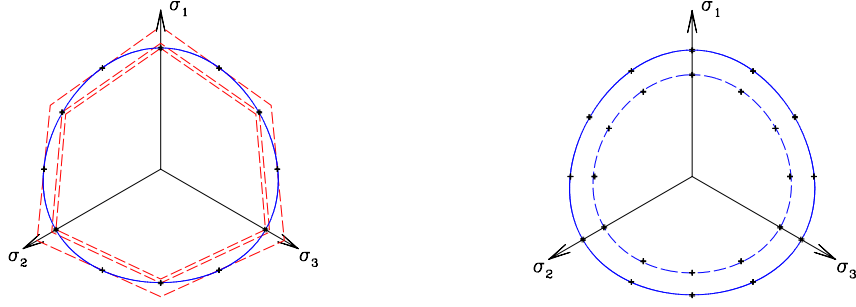


FIGURE 3. Failure criterion plotted in a deviatoric plane. Calculated failure points (in black) come with error bars. Left: comparison of a Lade-Duncan model (blue solid line) and a Mohr-Coulomb model (red dashed line) for $N = 1372$. Right: Lade-Duncan model for $N = 1372$ (solid line) and for $N = 4000$ (dashed line).

MICROSCOPIC ASPECTS

The network connectivity, the fabric tensor, the distribution of the values of contact forces and the orientational distribution of contact forces ([4]) have been investigated. On the one end, the network connectivity and the distribution of the values of the contact forces remain the same as in the isotropic case. On the other hand, the fabric tensor and the orientational contact forces distribution are anisotropic. At the lowest order, the orientational contact forces distribution may be expanded on the spherical harmonics of order two and the coefficients of the expansion are linked to the entries of the second-rank tensor $\underline{\underline{C}} = \int d\Omega f(\theta, \phi) \underline{n} \otimes \underline{n}$, where f is the averaged force and \underline{n} is the unit vector along the direction (θ, ϕ) . $\underline{\underline{F}} - 1/3 \underline{\underline{1}}$ and $\underline{\underline{C}} - 1/3 \underline{\underline{1}}$ ($1/3 \underline{\underline{1}}$ corresponds to the isotropic case) are dominated in the quasistatic limit by a single entry: F_{12} and C_{12} in the case of shear simulations in the 1-2 plane, $F_{33} - 1/3$ and $C_{33} - 1/3$ for triaxial test simulations along axis 3. Using the general expression of the stress tensor of a static packing ($\underline{\underline{\sigma}} = \frac{1}{V} \sum_{i < j} \underline{F}_{ij} \otimes \underline{r}_{ij}$, with V the sample volume, \underline{F}_{ij} the force between two grains in contact and \underline{r}_{ij} the vector joining the two centers of the touching grains) and performing a few approximations, one can show that:

- $\sigma_{12}/\sigma_{22} \simeq 3(F_{12} + C_{12})$ for a shear experiment;
- $\sigma_{33}/\sigma_{11} \simeq 2(F_{33} + C_{33} - 1/3)/(4/3 - F_{33} - C_{33})$ for a triaxial test.

According to numerical simulations, these equations, which link a macroscopic quantity (a stress component ratio) to microscopic data, work well: the discrepancy between the approximation and the actual ratio is always below 2%).

CONCLUSION

The macroscopic geometric limit of an assembly of spherical equal-sized frictionless beads was studied thanks to a detailed parametric study. Boundary conditions were shown to have no impact on the constitutive laws of the material. Quite strikingly, the material is devoid of dilatancy in this limit. A size-dependent Lade-Duncan failure criterion was evidenced by submitting the material to three different static loads (shear, triaxial compression and extension) and we observed that the static macroscopic friction coefficient coincide with the dynamic one in the macroscopic geometric limit. In the near future, we intend to simulate dense lubricated suspensions and to compare the results obtained with those presented in this work.

REFERENCES

1. N. Xu and C. S. O'Hern, Physical Review E **73**, 061303 (2006).
2. T. Hatano, Physical Review E **75**, 060301(R) (2007).
3. P.-E. Peyneau and J.-N. Roux, preprint [arXiv:0802.1502](https://arxiv.org/abs/0802.1502).
4. E. Azéma, F. Radjaï, R. Peyroux, and G. Saussine, Phys. Rev. E **76** (2007).